



Advanced multifunctional properties of aligned carbon nanotube-epoxy thin film composites



Peng Liu, Adriel Lam, Zeng Fan, Thang Q. Tran, Hai M. Duong*

Department of Mechanical Engineering, National University of Singapore, 9 Engineering Drive 1, EA-07-05, Singapore 117575, Singapore

ARTICLE INFO

Article history:

Received 29 May 2015

Received in revised form 3 August 2015

Accepted 16 August 2015

Available online 22 August 2015

Keywords:

Carbon nanotubes

Composites

Floating catalyst chemical vapor deposition

Resin transfer molding

Mechanical properties

Electrical properties

ABSTRACT

Carbon nanotube (CNT)/epoxy composite films were successfully developed by a combination of layer-by-layer and vacuum-assisted resin transfer molding methods using directly chemical vapor deposition (CVD)-spun CNT plies. CNT fractions in the composite films were found to be dramatically enhanced as the number of CNT plies increased. The as-prepared CNT/epoxy composite films with 24.4 wt.% CNTs exhibited ~10 and ~5 times enhancements in their strength and Young's modulus, respectively, and high toughness of up to 6.39×10^3 kJ/m³. Electrical conductivity reached 252.8 S/cm for the 20-ply CNT/epoxy films, which was 20 times higher over those of the CNT/epoxy composites obtained by conventional dispersion methods. This work proposed a route to fabricate high-CNT-fraction CNT/epoxy composites on a large scale. The high toughness of these CNT/epoxy composite films also makes them promising candidates as protective materials.

© 2015 Elsevier Ltd. All rights reserved.

1. Introduction

Carbon nanotubes (CNTs), with remarkable multifunctional properties, such as high strength and Young's modulus of 100 GPa and 1 TPa [1–3], respectively, ultrahigh electrical conductivity of 3×10^4 S/cm [4, 5] and outstanding thermal conductivity of 2000–3500 W/m·K [6,7], have attracted great attention over past few decades. CNTs have been regarded as promising reinforcements for developing high-performance multifunctional composites. However, due to the low volume fraction, poor dispersion and random orientation of the CNTs in matrices, most resultant CNT-based composites can only receive limited enhancements and exhibit properties much lower than expected [8,9]. To overcome these challenges, various CNT preforms, such as buckypapers [10], CNT arrays [11–13] and CNT yarns [14], have been developed to pre-arrange the CNTs in a pre-forming structure before preparing composites.

One traditional approach is to extract CNT films from CNT suspensions via solvent evaporation or vacuum-assisted filtration [15,16]. As surfactants and sonication are commonly involved to achieve a good dispersion of CNTs, the CNTs dispersed would usually suffer from inevitable damages or shortenings during this process, and the CNT orientation is also uncontrollable. Towards taking full advantages of the anisotropic properties of individual CNTs, a number of studies focused on the developments of aligned CNT architectures and aligned CNT polymer composites. Many previous works have shown that the well-

aligned CNTs could facilitate higher CNT packing densities and yield greater property enhancements in the composites than their tangled configurations [11–13,17–22]. So far, most aligned CNT preforms are fabricated from the CNT arrays [11–13] or dry-drawn CNT films from aligned CNT arrays [23]. Wardle et al. [11] reported the densification of CNT arrays reaching a high CNT volume fraction of up to ~20%, which nearly approached the theoretical limit of the intertube spacing in CNT arrays. Jiang et al. [24] reported a dry-drawing method to produce CNT sheets by directly pulling out the CNTs from CNT arrays. These as-prepared CNT sheets were further applied to fabricate CNT/epoxy composites which demonstrated improvements of 716% and 160% respectively in their Young's modulus and strength compared with pure epoxy [25]. Although these array-based methods provide a higher CNT content in the composites, a scaled-up fabrication is still restrained by the low production and the limited size of the CNT arrays [26].

Recently, continuous and large-scaled CNT sheets have been successfully synthesized via a floating catalytic chemical vapor deposition (FC-CVD) method [27,28]. In this process, aligned CNT sheets with controlled thickness and dimensions can be directly collected from the self-assembled CNT aerogels in the CVD furnace. Song et al. [29] reported CVD-grown CNT films with lateral dimensions of several tens of square centimeters, which exhibited Young's moduli of up to 700 GPa. By a similar approach, Ma et al. [30] produced strong and highly conducting films, which possessed strength of 360 MPa and electrical conductivity of over 2000 S/cm. Feng et al. [31] reported a one-step fabrication of double-walled CNT films and further enhanced their electrical conductivity to approximately 8000 S/cm. Such direct CVD-grown

* Corresponding author.

E-mail address: mpedhm@nus.edu.sg (H.M. Duong).

method, therefore, not only provides an effective way to fabricate CNT films on a large scale, but also favors the fabrication of unidirectional CNT-based composites in a mass production.

Resin transfer molding (RTM) is a very common and cost-effective method to fabricate composites in industries, in which the liquid resins are first injected to the preforms and then cured to be solid [25,32,33]. Given its capability of making composites with large sizes and complex shapes, RTM is expected to be appropriate for preparing large-scaled CNT/epoxy composites using the CVD-grown CNT films. For the as-prepared CNT/epoxy composite films, understanding the effects of CNT-ply numbers on their multifunctional properties can also provide a basis for the optimization of their properties.

In this work, we report a simple yet controllable strategy to fabricate large-scaled CNT/epoxy composite films. The multi-ply CNT films were prepared by uniaxially stacking 1, 5, 10 and 20 CNT plies, which were continuously collected from CNT aerogels via FC-CVD. The CNT/epoxy composite films with high CNT volume fractions were readily obtained through a following vacuum-assisted resin transfer molding (VA-RTM) process. Multifunctional properties of these as-prepared CNT/epoxy films were characterized as a function of the numbers of their CNT plies. This work reports a novel approach to prepare high-volume-fraction CNT-based composites, and also seeks to identify the factors limiting their mechanical performance.

2. Experimental section

2.1. Materials

Ferrocene, thiophene and ethanol were purchased from Sigma-Aldrich Company Ltd. Methane, hydrogen and helium were purchased from Chem-Gas Pte Ltd. Epicote 1004 epoxy resin and Epicote 1004 hardener were obtained from Polymer Technologies. All the chemicals above were used as received.

2.2. Fabrication of CNT films

CNT films were synthesized via a FC-CVD method [34]. A mixture of methane (CH_4), hydrogen (H_2), ferrocene and thiophene was injected into a heated reactor at $1200\text{ }^\circ\text{C}$ under nitrogen (N_2) environment. CNT aerogels were continuously formed at the heating region, blown out by the carrier gas and wound on a roller to form the CNT films, as

shown in Fig. 1(a). In this work, an as-rolled CNT film from a 10-min continuous collection was defined as 1 CNT ply. Multiple CNT plies (containing 5, 10 and 20 individual CNT plies) were then stacked in the same CNT direction to form the CNT preforms, as shown in Fig. 1(b).

2.3. Fabrication of CNT/epoxy composite films

To fabricate the CNT/epoxy composite films, the as-prepared CNT films above were first placed in a self-made RTM mold, and then the epoxy resin was allowed to pass through the CNT films under vacuum. As recommended by the manufacturer, the mix ratio of Epicote 1004 and Epicote 1004 hardener was in a weight ratio of 5:2, while the curing condition was at the room temperature for 24 h. In order to minimize the air bubbles in the composite films, loads of $\sim 20\text{ kg}$ were placed on the top of the molds during curing. CNT/epoxy composite films were eventually obtained by carefully releasing the samples from the RTM mold, as the process illustrated in Fig. 1(c)–(d). In order to investigate the effects of CNT-ply numbers, CNT/epoxy films with 1, 5, 10 and 20 CNT plies were prepared.

2.4. Characterization

Tensile tests were conducted along the CNT direction on an Instron 5500 tensile tester. Gauge length and crosshead speed were set to 15 mm and 1.5 mm/min, respectively. Thickness of the films was measured by a micrometer. Mechanical properties of these films were finally obtained by testing at least three samples at ambient conditions.

Theoretically, effective mechanical properties of the CNT films could be calculated from a modified rule of mixtures (ROM) [9,25] as below:

$$E_c = \eta_0 \cdot \eta_L \cdot V_f \cdot E_f + (1 - V_f) \cdot E_m \quad (1)$$

$$\sigma_c = \eta_0 \cdot \eta_L \cdot V_f \cdot \sigma_f + (1 - V_f) \cdot \sigma_m \quad (2)$$

where E_c , E_m and E_f and σ_c , σ_m and σ_f are Young's modulus and strength of composite, epoxy and CNTs, respectively. η_L and η_0 are introduced as length efficient factor and CNT orientation factor respectively, both of which could be set to be 1 for aligned CNTs with a high aspect ratio.

After the tensile tests, fracture surfaces of the composite films were coated with gold and subjected to field emission scanning electron microscope (FE-SEM, Model S-4300, Hitachi, Japan) to investigate their

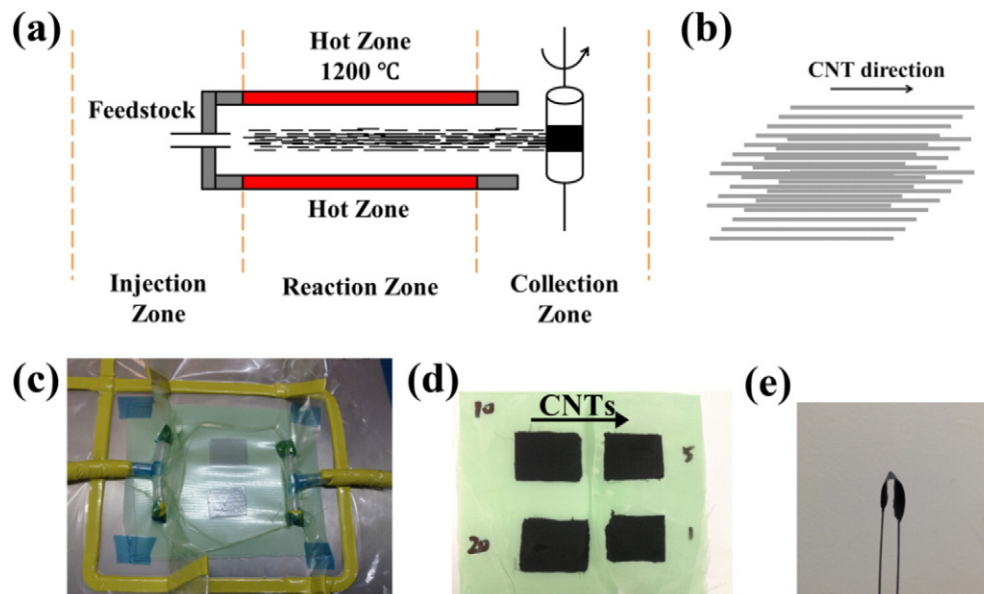


Fig. 1. Fabrication process of the CNT/epoxy films. (a) Schematic illustration of the fabrication of CNT plies by a FC-CVD method. (b) Schematic illustration of the arrangement of CNT plies. (c) Experimental set-up of the RTM process for preparing CNT/epoxy films. (d) As-prepared CNT/epoxy films with 1, 5, 10 and 20 CNT plies. (e) A flexible CNT/epoxy film bent by tweezers.

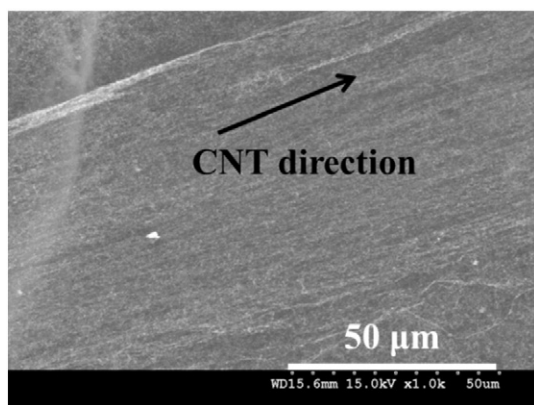


Fig. 2. An SEM image of the as-prepared CNT ply.

fracture morphology. To evaluate the CNT weight fractions in the composite films, thermogravimetric analysis (TGA) was conducted on an SDT Q600 thermo gravimetric analyzer from room temperature to 1000 °C in nitrogen with a heating rate of 10 °C/min.

Electrical property of the CNT/epoxy composite films was tested by a two-probe method using a multimeter (Fluke 73III). Two ends of the composite films were separately fixed on two glass slides with a distance between of 1.5 cm. Silver paste was applied to ensure good electrical contacts between the test films and electrodes. Electrical conductivities of all the CNT/epoxy composite films were measured in the direction parallel to the CNT alignment.

3. Results and discussion

3.1. Morphology of CNT/epoxy films

Fig. 2 shows a SEM image of the as-prepared CNT ply with a good CNT alignment. The as-prepared CNT/epoxy films containing 1, 5, 10 and 20 CNT plies all have a lateral dimension of 4 cm × 3 cm, while their thickness monotonically increase with the number of CNT plies, as shown in Table 1. Compared with the pure epoxy film of 70.2 μm, CNT/epoxy films with 1, 5, 10 and 20 CNT plies possess greater thicknesses of 101.9, 128.5, 223.3 and 267.7 μm. Evidently, the increments of the film thicknesses are shown to be inferior, compared with the simple multiplication of the thickness of several 1-ply CNT/epoxy films. For example, the thickness of the 20-ply CNT/epoxy film is only twice that of the 1-ply CNT/epoxy film. Therefore, the CNT plies involved in the CNT/epoxy films are speculated to be effectively condensed during the fabrication processes. Notably, as all the as-prepared CNT/epoxy films are very thin in thickness, a good flexibility is still observable. As shown in Fig. 1(e), the film is found to be easily bent to a radius of several millimeters by a pair of tweezers.

Table 1
Properties of the CNT/epoxy composite films.

Property	Pure epoxy	CNT/epoxy composite films			
		1-ply	5-ply	10-ply	20-ply
Thickness (μm)	70.2 ± 2.2	101.9 ± 9.4	128.5 ± 7.4	223.3 ± 19.4	267.7 ± 8.3
CNT mass fraction (wt.%)	0	5.1	15.0	20.9	24.4
CNT volume fraction* (vol.%)	0	3.1	9.6	13.7	16.2
Electrical conductivity (S/cm)	–	44.3 ± 5.6	161.7 ± 25.4	187.9 ± 18.5	252.8 ± 35.8
Young's modulus (GPa)	1.14 ± 0.15	1.14 ± 0.26	2.94 ± 0.05	3.62 ± 0.44	5.28 ± 0.28
Tensile strength (MPa)	15.35 ± 2.27	16.12 ± 5.45	67.04 ± 6.77	89.27 ± 11.71	143.71 ± 8.96
Tensile toughness (× 10 ³ kJ/m ³)	0.14 ± 0.01	0.11 ± 0.01	2.08 ± 0.01	2.50 ± 0.31	6.39 ± 0.19

* Densities for calculation: epoxy 1.2 g/cm³, CNT 2 g/cm³.

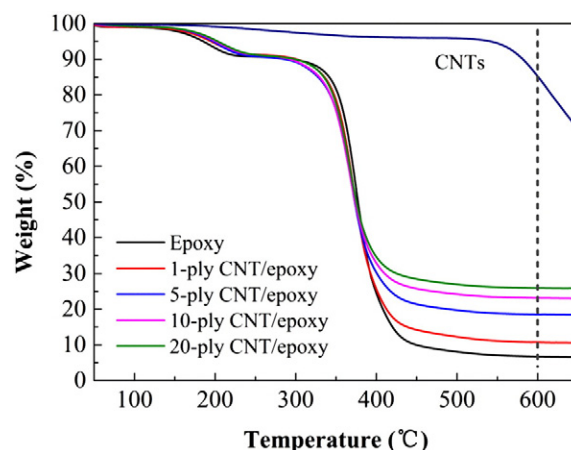


Fig. 3. TGA curves of pure CNT films, pure epoxy and CNT/epoxy films with 1, 5, 10 and 20 CNT plies.

CNT weight fractions in these CNT/epoxy films were determined by their TGA curves [35,36], as displayed in Fig. 3. From the results obtained at 600 °C, CNT weight fractions in the 1-, 5-, 10 and 20-ply CNT/epoxy films are calculated to be 5.1, 15.0, 20.9 and 24.4 wt.%, respectively, further indicating the CNT condensations in the VA-RTM process. The CNT weight fractions and the thickness of CNT/epoxy composite films are plotted in Fig. 4 as a function of thickness of CNT plies.

3.2. Mechanical properties of CNT/epoxy films

Fig. 5 shows typical stress–strain curves of the CNT/epoxy films with different CNT plies. Table 1 summarizes the Young's modulus and tensile strength of these films. As the increase of CNT plies, CNT/epoxy films exhibit a dramatic enhancement in their modulus and strength. The 1-ply CNT/epoxy film containing 5.1 wt.% CNTs only possesses a 1.14 GPa modulus and 16.12 MPa strength, slightly higher than the pure epoxy film, while the 5-, 10- and 20-ply CNT/epoxy films show significantly higher moduli of 2.94, 3.62 and 5.28 GPa, and higher strengths of 67.04, 89.27 and 143.71 MPa, respectively. As the CNT plies are increased in the CNT/epoxy films, such great improvement is probably contributed by the increased CNT weight fractions and denser CNT packing. During the layering and RTM processes, CNT plies are mechanically pressed and infiltrated by epoxy under vacuum, which therefore greatly reduce the porosity within the resultant films and also generate good CNT–CNT and CNT–epoxy contacts.

As the volume densities of these CNT/epoxy films increase with higher CNT weight fractions, the enhanced interactions between CNT–epoxy and inter-tubes would largely benefit the load transfer under external tensile stresses. Besides, the utilization of a VA-RTM process has shown to be an effective way for eliminating air bubbles in the composites [25]. These results above indicate that our layering and the RTM

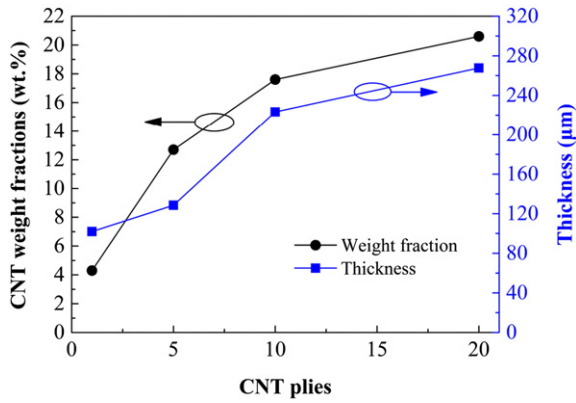


Fig. 4. The CNT weight fractions and the thickness of CNT/epoxy composite films as a function of CNT plies.

method could successfully achieve an effective load transfer between the CNT plies and epoxy. For the 20-ply CNT/epoxy film, its gravimetric strength is converted to be $150 \text{ MPa}/(\text{g}/\text{cm}^3)$, which is significantly higher than the steel alloy 1040 ($75 \text{ MPa}/(\text{g}/\text{cm}^3)$), and comparable to the CNT/epoxy composite films ($180 \text{ MPa}/(\text{g}/\text{cm}^3)$) prepared by a similar RTM process yet using continuously drawn CNT sheets [25].

As shown in Fig. 5 and Table 1, ductility (fracture strain) and tensile toughness (area under stress–strain curves) of these CNT/epoxy films also exhibit an increasing tendency with the increase of CNT plies. From the 1-ply to 20-ply CNT/epoxy composite films, their toughness ranges from 0.11×10^3 to $6.39 \times 10^3 \text{ kJ}/\text{m}^3$, corresponding to the ductility from 1.33 to 6.38%. Compared with that of the pure epoxy film ($0.14 \times 10^3 \text{ kJ}/\text{m}^3$), toughness of the 1-ply CNT/epoxy composite films shows a slightly lower decrease due to the cross-linked network formed by epoxy molecules. However, for the CNT/epoxy films having more than 5 CNT plies, plastic behaviors with increased toughness could be apparently observed in their stress–strain curves (See Fig. 5 and Table 1). As reported by Jiang et al. [37], CNTs and epoxy commonly play the roles of main constitute and adhesive respectively in the composites with high CNT loadings, and their ductility is largely determined by the CNT assemblies. For this reason, the high ductility and toughness of the multi-ply CNT/epoxy films may probably be results of the presence of numerous CNT junctions and the occurrence of enormous slippage between inter-tubes and CNT bundles [26]. However, the tensile toughness here may reveal no direct synergism with the fracture toughness (K_{IC}) [38]. Future work could deeply investigate the fracture behavior of these multi-ply CNT/epoxy films as a function of CNT plies.

Fig. 6 compares the fracture surfaces of the 1-ply and 20-ply CNT/epoxy composite films, in which a 4-time longer pullout distance is

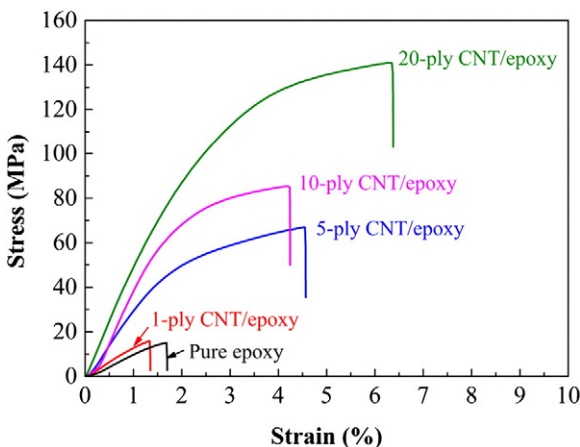


Fig. 5. Typical tensile stress–strain curves of CNT/epoxy films with different CNT plies.

clearly observed for the 20-ply film, consistent with the improvement in ductility. With the presence of CNT bundles, a plastic shear yielding of the epoxy may also be a possible reason for the plastic deformation [39]. Considering the fabrication process of combining layer-by-layer (LBL) and VA-RTM, the structure of the CNT/epoxy films developed in this work may be close to the laminated composite structure as reported by Mirjalili et al. [40]. Above all, the CNT/epoxy films in this work exhibit good flexibility and high toughness, which could make them promising candidates as protective materials and also structural materials that are sensitive to catastrophic failure [41–43].

3.3. Fracture mechanisms

As the stress–strain curves shown in Fig. 5, the deformation behavior of a CNT/epoxy film includes different stages of elastic, plastic and damage–fracture [44]. As tensile loading is applied from 0, the film first exhibits the elastic deformation governed by the elastic behavior of individual CNTs and epoxy matrix. As the loading increases, the plastic deformation is then observed; it is mainly caused by the slippage among CNTs and the plastic deformation of epoxy-coated CNT bundles. With the accumulation of slippage and further increase of the external loading, fracture of the composite film finally occurs. Fig. 7 presents the elastic modulus and tensile strength as a function of CNT volume fraction. The best fit Young's modulus and strength of CNTs are extracted to be 22.58 GPa and 665.97 MPa respectively, according to Eqs. (1) and (2). These values are at least one order lower than the theoretical Young's modulus and strength of individual CNTs. Given this concern, the inferior mechanical properties of the composite films may probably be ascribed to multiple fracture mechanisms.

First, the perfect load transfer between CNTs and matrix could never be fulfilled, and CNT pullouts and CNT fracture would constantly occur upon the external tensile loadings [45]. As epoxy molecules have penetrated and cross-linked through the entire CNT preforms, an epoxy coating is commonly formed on the surface of CNT bundles. Interfacial debondings, therefore either as CNT fracture or CNT pullouts [46], would be generated between the matrix and epoxy-coated CNT bundles [47], rather than between the matrix and individual CNTs. In this case, an improvement of the interfacial adhesion between CNT preforms and matrices, such as functionalization of CNTs or selection of polymers as matrices, may be an effective approach to increase the load transfer efficiency within the composites [48].

Second, the CVD-grown CNT films usually possess high strains but low Young's moduli and strengths due to their unsatisfactory CNT alignment [26,49]. Meanwhile, the waviness of the CNTs would also restrain the completely straightening of CNTs, thus limiting the stress transfer along the tensile direction [50]. Our future work is going to involve pre-stretching to the as-prepared CNT films, which is believed to readily prompt the anisotropic property of the CNT films as well as that of the resultant CNT/epoxy composite films.

In addition, the quality of CNTs also plays an important role in the mechanical properties of the composites. Based on the observation of interfacial fracture under TEM, several types of defects have been detected [47]. Typically, the embedded metallic catalyst and the disordered CNT structures would easily cause stress concentration, while the large diameter and multi-walls of the CNTs would lead to a sword-in-sheath failure [9]. Additionally, the excessive epoxy layers on both sides of the true effective composite region could also decline the mechanical properties of the composite by up to 60% [51], which, however, might not be significant in this work due to the mechanically pressing during the VA-RTM process.

3.4. Electrical properties of CNT/epoxy films

Electrical conductivities of the CNT/epoxy films are shown in Table 1 and Fig. 8. Epicoate 1004 epoxy is intrinsically an insulator, having the electrical conductivity of $\sim 10^{-12} \text{ S}/\text{cm}$ [25]. When increasing the CNT

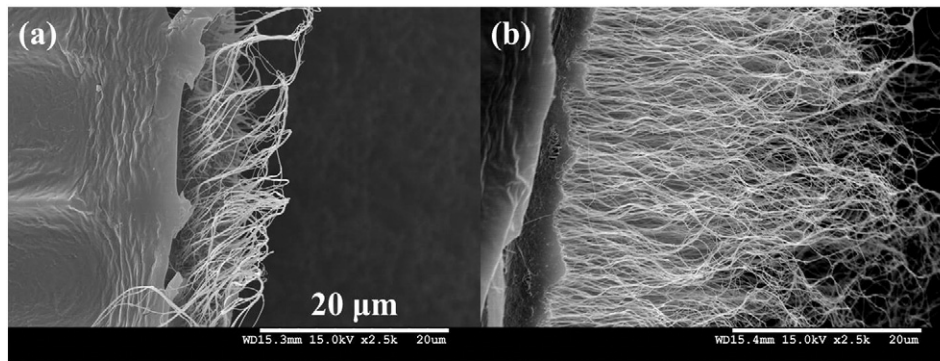


Fig. 6. SEM images of (a) 1-ply and (b) 20-ply CNT/epoxy composite films after tensile test.

plies from 1 to 20, the electrical conductivities of the CNT/epoxy films show a great improvement from 44.3 to 252.8 S/cm. The highest conductivity of 252.8 S/m, obtained at 24.4 wt.% CNTs (20-ply CNTs), is ~1.6 times higher than that of the CNT/PVA films at 20 wt.% CNTs prepared by a spray winding process [52], and much higher than those of the CNT/epoxy composites obtained by conventional dispersion methods (generally less than 10 S/cm) [53–55]. Such remarkably enhanced electrical conductivity with the increase of CNT plies could be attributed to the increased CNT fractions and the well-preserved CNT alignments during the layering and RTM processes. It can be expected that as a further increase of CNT plies, the CNT/epoxy films with even higher electrical conductivities could be obtained. In addition,

our method is also capable of being further improved by combining various pre-treatments, such as pre-stretching and hot-pressing.

4. Conclusions

A combination of layer-by-layer and vacuum-assisted resin transfer molding method was used in this work to develop CNT/epoxy composite films containing 1, 5, 10 and 20 CNT plies. It was found that CNT fractions in the composite films could be easily controlled by altering the number of CNT plies. A maximum CNT fraction of 24.4 wt.% (16.2 vol.%) has been successfully achieved by 20-ply CNT/epoxy composite films, which overcomes the inter-CNT spacing for aligned CNT arrays. Compared with pure epoxy films, these as-prepared CNT/epoxy composite films exhibited good mechanical properties, up to ~10 and ~5 times enhancements in their strength and Young's modulus, respectively. Unlike most other CNT/epoxy composites, the composite films developed in this work also showed increased toughness from 0.11×10^3 to 6.39×10^3 kJ/m³. Besides, a significant improvement in electrical conductivities from 44.3 to 252.8 S/cm has also been obtained. This work provides a facile approach to fabricate CNT/epoxy composite films on a large scale, and also paves the way to effectively increase CNT fractions in the composites. The CNT/epoxy composite films obtained in this work would be a promising candidate as protective materials due to their high toughness, and may also help to better understand the CNT laminated composites.

Acknowledgments

The authors deeply acknowledge the Defence Research and Technology of MINDEF (R-394-001-077-232) for funding support. The authors also thank Dr. Nguyen Truong Son for his help on language modification.

References

- [1] M.S. Dresselhaus, G. Dresselhaus, R. Saito, Carbon fibers based on C60 and their symmetry, *Phys. Rev. B* 45 (1992) 6234–6242.
- [2] M. Yu, O. Lourie, M.J. Dyer, K. Moloni, T.F. Kelly, R.S. Ruoff, Strength and breaking mechanism of multiwalled carbon nanotubes under tensile load, *Science* 287 (2000) 637–640.
- [3] B.G. Demczyk, Y.M. Wang, J. Cumings, M. Hetman, W. Han, A. Zettl, R.O. Ritchie, Direct mechanical measurement of the tensile strength and elastic modulus of multiwalled carbon nanotubes, *Mater. Sci. Eng. A* 334 (2002) 173–178.
- [4] Q.W. Li, Y. Li, X.F. Zhang, S.B. Chikkannanavar, Y.H. Zhao, A.M. Danglewicz, L.X. Zheng, S.K. Doorn, Q.X. Jia, D.E. Peterson, P.N. Arendt, Y.T. Zhu, Structure-dependent electrical properties of carbon nanotube fibers, *Adv. Mater.* 19 (2007) 3358–3363.
- [5] P.G. Collins, P. Avouris, Nanotubes for electronics, *Sci. Am.* 283 (2000) 62–69.
- [6] E. Pop, D. Mann, Q. Wang, K. Goodson, H. Dai, Thermal conductance of an individual single-wall carbon nanotube above room temperature, *Nano Lett.* 6 (2005) 96–100.
- [7] P. Kim, L. Shi, A. Majumdar, P.L. McEuen, Thermal transport measurements of individual multiwalled nanotubes, *Phys. Rev. Lett.* 87 (2001) 215502.
- [8] T. Tsuda, T. Ogasawara, S.-Y. Moon, K. Nakamoto, N. Takeda, Y. Shimamura, Y. Inoue, Three dimensional orientation angle distribution counting and calculation for the mechanical properties of aligned carbon nanotube/epoxy composites, *Compos. A: Appl. Sci. Manuf.* 65 (2014) 1–9.

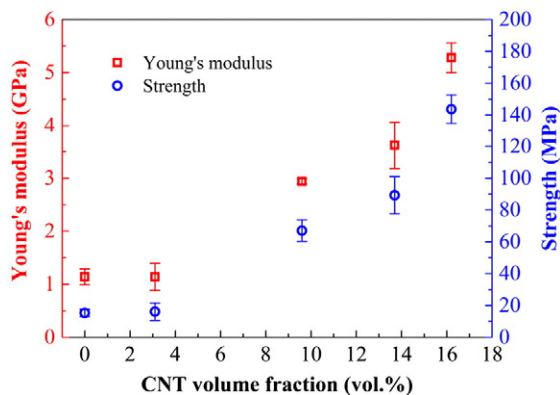


Fig. 7. Strength and Young's modulus of CNT/epoxy composite films as a function of CNT volume fraction.

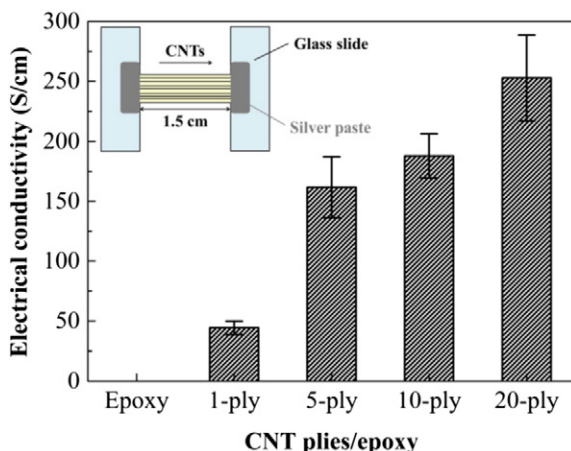


Fig. 8. Electrical conductivity of the CNT/epoxy films as a function of CNT plies.

- [9] T. Ogasawara, S.-Y. Moon, Y. Inoue, Y. Shimamura, Mechanical properties of aligned multi-walled carbon nanotube/epoxy composites processed using a hot-melt prepreg method, *Compos. Sci. Technol.* 71 (2011) 1826–1833.
- [10] D. Vennerberg, M.R. Kessler, Anisotropic buckypaper through shear-induced mechanical alignment of carbon nanotubes in water, *Carbon* 80 (2014) 433–439.
- [11] B.L. Wardle, D.S. Saito, E.J. Garcia, A.J. Hart, R.G. de Villoria, E.A. Verploegen, Fabrication and characterization of ultrahigh-volume-fraction aligned carbon nanotube-polymer composites, *Adv. Mater.* 20 (2008) 2707–2714.
- [12] H. Becabi, R.G. de Villoria, A.J. Hart, B.L. Wardle, Multifunctional properties of high volume fraction aligned carbon nanotube polymer composites with controlled morphology, *Compos. Sci. Technol.* 69 (2009) 2649–2656.
- [13] E.J. Garcia, A.J. Hart, B.L. Wardle, A.H. Slocum, Fabrication and nanocompression testing of aligned carbon-nanotube-polymer nanocomposites, *Adv. Mater.* 19 (2007) 2151–2156.
- [14] K. Jiang, Q. Li, S. Fan, Nanotechnology: spinning continuous carbon nanotube yarns, *Nature* 419 (2002) 801.
- [15] Z. Wang, Z. Liang, B. Wang, C. Zhang, L. Kramer, Processing and property investigation of single-walled carbon nanotube (SWNT) buckypaper/epoxy resin matrix nanocomposites, *Compos. A: Appl. Sci. Manuf.* 35 (2004) 1225–1232.
- [16] Z. Spitalsky, G. Tsoukleri, D. Tasis, C. Krontiras, S.N. Georga, C. Galiotis, High volume fraction carbon nanotube-epoxy composites, *Nanotechnology* 20 (2009) 405702.
- [17] L. Liu, W. Ma, Z. Zhang, Macroscopic carbon nanotube assemblies: preparation, properties, and potential applications, *Small* 7 (2011) 1504–1520.
- [18] A.T. Sepulveda, R. Guzman de Villoria, J.C. Viana, A.J. Pontes, B.L. Wardle, L.A. Rocha, Full elastic constitutive relation of non-isotropic aligned-CNT/PDMS flexible nanocomposites, *Nanoscale* 5 (2013) 4847–4854.
- [19] A.M.K. Esawi, M.M. Farag, Carbon nanotube reinforced composites: potential and current challenges, *Mater. Des.* 28 (2007) 2394–2401.
- [20] J. Huang, D. Rodrigue, Equivalent continuum models of carbon nanotube reinforced polypropylene composites, *Mater. Des.* 50 (2013) 936–945.
- [21] Z. Cai, X. Meng, H. Ye, C. Cong, Y. Wang, L. Cui, Q. Zhou, Reinforcing polyamide 1212 nanocomposites with aligned carbon nanofibers, *Mater. Des.* 63 (2014) 691–698.
- [22] J. Yan, Y.G. Jeong, Highly elastic and transparent multiwalled carbon nanotube/polydimethylsiloxane bilayer films as electric heating materials, *Mater. Des.* 86 (2015) 72–79.
- [23] M. Zhang, K.R. Atkinson, R.H. Baughman, Multifunctional carbon nanotube yarns by downsizing an ancient technology, *Science* 306 (2004) 1358–1361.
- [24] K. Liu, Y. Sun, L. Chen, C. Feng, X. Feng, K. Jiang, Y. Zhao, S. Fan, Controlled growth of super-aligned carbon nanotube arrays for spinning continuous unidirectional sheets with tunable physical properties, *Nano Lett.* 8 (2008) 700–705.
- [25] Q.F. Cheng, J.P. Wang, J.J. Wen, C.H. Liu, K.L. Jiang, Q.Q. Li, S.S. Fan, Carbon nanotube/epoxy composites fabricated by resin transfer molding, *Carbon* 48 (2010) 260–266.
- [26] Q. Liu, M. Li, Y. Gu, Y. Zhang, S. Wang, Q. Li, Z. Zhang, Highly aligned dense carbon nanotube sheets induced by multiple stretching and pressing, *Nanoscale* 6 (2014) 4338–4344.
- [27] Y.-L. Li, I.A. Kinloch, A.H. Windle, Direct spinning of carbon nanotube fibers from chemical vapor deposition synthesis, *Science* 304 (2004) 276–278.
- [28] K. Koziol, J. Vilatela, A. Moiala, M. Motta, P. Cuniff, M. Sennett, A. Windle, High-performance carbon nanotube fiber, *Science* 318 (2007) 1892–1895.
- [29] L. Song, L. Ci, L. Lv, Z. Zhou, X. Yan, D. Liu, H. Yuan, Y. Gao, J. Wang, L. Liu, X. Zhao, Z. Zhang, X. Dou, W. Zhou, G. Wang, C. Wang, S. Xie, Direct synthesis of a macroscale single-walled carbon nanotube non-woven material, *Adv. Mater.* 16 (2004) 1529–1534.
- [30] W. Ma, L. Song, R. Yang, T. Zhang, Y. Zhao, L. Sun, Y. Ren, D. Liu, L. Liu, J. Shen, Z. Zhang, Y. Xiang, W. Zhou, S. Xie, Directly synthesized strong, highly conducting, transparent single-walled carbon nanotube films, *Nano Lett.* 7 (2007) 2307–2311.
- [31] J.-M. Feng, R. Wang, Y.-L. Li, X.-H. Zhong, L. Cui, Q.-J. Guo, F. Hou, One-step fabrication of high quality double-walled carbon nanotube thin films by a chemical vapor deposition process, *Carbon* 48 (2010) 3817–3824.
- [32] O. Restrepo, K.-T. Hsiao, A. Rodriguez, B. Minaie, Development of adaptive injection flow rate and pressure control algorithms for resin transfer molding, *Compos. A: Appl. Sci. Manuf.* 38 (2007) 1547–1568.
- [33] S. Rwawiire, B. Tomkova, Thermal, static, and dynamic mechanical properties of bark cloth (*ficus brachypoda*) laminar epoxy composites, *Polym. Compos.* (2015) <http://dx.doi.org/10.1002/pc.23576>.
- [34] P. Liu, T.Q. Tran, Z. Fan, H.M. Duong, Formation mechanisms and morphological effects on multi-properties of carbon nanotube fibers and their polyimide aerogel-coated composites, *Compos. Sci. Technol.* 117 (2015) 114–120.
- [35] Y.-N. Liu, M. Li, Y. Gu, K. Wang, D. Hu, Q. Li, Z. Zhang, A modified spray-winding approach to enhance the tensile performance of array-based carbon nanotube composite films, *Carbon* 65 (2013) 187–195.
- [36] X. Wang, Z.Z. Yong, Q.W. Li, P.D. Bradford, W. Liu, D.S. Tucker, W. Cai, H. Wang, F.G. Yuan, Y.T. Zhu, Ultrastrong, stiff and multifunctional carbon nanotube composites, *Math. Res. Lett.* 1 (2012) 19–25.
- [37] Q. Jiang, X. Wang, Y. Zhu, D. Hui, Y. Qiu, Mechanical, electrical and thermal properties of aligned carbon nanotube/polyimide composites, *Compos. Part B* 56 (2014) 408–412.
- [38] M. Abadyan, R. Bagheri, M.A. Kouchakzadeh, S.A. Hosseini Kordkheili, Exploring the tensile strain energy absorption of hybrid modified epoxies containing soft particles, *Mater. Des.* 32 (2011) 2900–2908.
- [39] T. Kawaguchi, R.A. Pearson, The moisture effect on the fatigue crack growth of glass particle and fiber reinforced epoxies with strong and weak bonding conditions: part 2. A microscopic study on toughening mechanism, *Compos. Sci. Technol.* 64 (2004) 1991–2007.
- [40] V. Mirjalili, R. Ramachandramoorthy, P. Hubert, Enhancement of fracture toughness of carbon fiber laminated composites using multi wall carbon nanotubes, *Carbon* 79 (2014) 413–423.
- [41] X. Zhang, Q. Li, T.G. Holesinger, P.N. Arendt, J. Huang, P.D. Kirven, T.G. Clapp, R.F. DePaula, X. Liao, Y. Zhao, L. Zheng, D.E. Peterson, Y. Zhu, Ultrastrong, stiff, and lightweight carbon-nanotube fibers, *Adv. Mater.* 19 (2007) 4198–4201.
- [42] X. Zhang, Q. Li, Y. Tu, Y. Li, J.Y. Coulter, L. Zheng, Y. Zhao, Q. Jia, D.E. Peterson, Y. Zhu, Strong carbon-nanotube fibers spun from long carbon-nanotube arrays, *Small* 3 (2007) 244–248.
- [43] G.H. Bratzel, S.W. Cranford, H. Espinosa, M.J. Buehler, Bioinspired noncovalently crosslinked “fuzzy” carbon nanotube bundles with superior toughness and strength, *J. Mater. Chem.* 20 (2010) 10465–10474.
- [44] L. Qiu, K. Yi-Lan, Q. Wei, L. Ya-Li, H. Gan-Yun, G. Jian-Gang, D. Wei-Lin, Z. Xiao-Hua, Deformation mechanisms of carbon nanotube fibres under tensile loading by in situ Raman spectroscopy analysis, *Nanotechnology* 22 (2011) 225704.
- [45] M. Zu, Q. Li, Y. Zhu, M. Dey, G. Wang, W. Lu, J.M. Deitzel, J.W. Gillespie Jr., J.-H. Byun, T.-W. Chou, The effective interfacial shear strength of carbon nanotube fibers in an epoxy matrix characterized by a microdroplet test, *Carbon* 50 (2012) 1271–1279.
- [46] M. Mecklenburg, D. Mizushima, N. Ohtake, W. Bauhofer, B. Fiedler, K. Schulte, On the manufacturing and electrical and mechanical properties of ultra-high wt.% fraction aligned MWCNT and randomly oriented CNT epoxy composites, *Carbon* 91 (2015) 275–290.
- [47] T. Tsuda, T. Ogasawara, Moon S-y, K. Nakamoto, N. Takeda, Y. Shimamura, Y. Inoue, Nanoscopic observations for evaluating the failure process of aligned multi-walled carbon nanotube/epoxy composites, *Compos. Sci. Technol.* 88 (2013) 48–56.
- [48] Z. Wang, X. Huang, G. Xian, H. Li, Effects of surface treatment of carbon fiber: tensile property, surface characteristics, and bonding to epoxy, *Polym. Compos.* (2015) <http://dx.doi.org/10.1002/pc.23489>.
- [49] T.H. Nam, K. Goto, H. Nakayama, K. Oshima, V. Premalal, Y. Shimamura, Y. Inoue, K. Naito, S. Kobayashi, Effects of stretching on mechanical properties of aligned multi-walled carbon nanotube/epoxy composites, *Compos. A: Appl. Sci. Manuf.* 64 (2014) 194–202.
- [50] N.J. Ginga, W. Chen, S.K. Sitaraman, Waviness reduces effective modulus of carbon nanotube forests by several orders of magnitude, *Carbon* 66 (2014) 57–66.
- [51] J. Li, Y. Gao, W. Ma, L. Liu, Z. Zhang, Z. Niu, Y. Ren, X. Zhang, Q. Zeng, H. Dong, D. Zhao, L. Cai, W. Zhou, S. Xie, High performance, freestanding and superthin carbon nanotube/epoxy nanocomposite films, *Nanoscale* 3 (2011) 3731–3736.
- [52] W. Liu, H. Zhao, Y. Inoue, X. Wang, P.D. Bradford, H. Kim, Y. Qiu, Y. Zhu, Poly(vinyl alcohol) reinforced with large-diameter carbon nanotubes via spray winding, *Compos. A: Appl. Sci. Manuf.* 43 (2012) 587–592.
- [53] J. Sandler, M.S.P. Shaffer, T. Prasse, W. Bauhofer, K. Schulte, A.H. Windle, Development of a dispersion process for carbon nanotubes in an epoxy matrix and the resulting electrical properties, *Polymer* 40 (1999) 5967–5971.
- [54] A. Allaoui, S. Bai, H.M. Cheng, J.B. Bai, Mechanical and electrical properties of a MWNT/epoxy composite, *Compos. Sci. Technol.* 62 (2002) 1993–1998.
- [55] A. Moiala, Q. Li, I.A. Kinloch, A.H. Windle, Thermal and electrical conductivity of single- and multi-walled carbon nanotube-epoxy composites, *Compos. Sci. Technol.* 66 (2006) 1285–1288.